Moduli vacuum bubbles produced by evaporating black holes

J. R. Morris

Physics Department, Indiana University Northwest, 3400 Broadway, Gary, Indiana 46408, USA

(Received 26 July 2006; revised manuscript received 16 July 2007; published 3 October 2007)

We consider a model with a toroidally compactified extra dimension giving rise to a temperature-dependent 4D effective potential with one-loop contributions due to the Casimir effect, along with a 5D cosmological constant. The forms of the effective potential at low and high temperatures indicate a possibility for the formation of a domain wall bubble, formed by the modulus scalar field, surrounding an evaporating black hole. This is viewed as an example of a recently proposed black hole vacuum bubble arising from matter-sourced moduli fields in the vicinity of an evaporating black hole [D. Green, E. Silverstein, and D. Starr, Phys. Rev. D **74**, 024004 (2006)]. The black hole bubble can be highly opaque to lower-energy particles and photons, and thereby entrap them within. For high-temperature black holes, there may also be a symmetry-breaking black hole bubble of false vacuum of the type previously conjectured by Moss [I. G. Moss, Phys. Rev. D **32**, 1333 (1985)], tending to reflect low-energy particles from its wall. A double bubble composed of these two different types of bubble may form around the black hole, altering the hole's emission spectrum that reaches outside observers. Smaller mass black holes that have already evaporated away could have left vacuum bubbles behind that contribute to the dark matter.

DOI: 10.1103/PhysRevD.76.085003 PACS numbers: 11.27.+d, 04.50.+h, 98.80.Cq

I. INTRODUCTION

A black hole freely radiating into empty space through the Hawking process [1] has an associated temperature $T_h = 1/(8\pi G M_h)$ where M_h is the mass of the black hole. The evaporation rate is inversely proportional to the mass, $\dot{M}_h \propto -1/(GM_h)^2$, so that primordial black holes (PBHs) created soon after the big bang with masses $M_h \lesssim 10^{12}$ kg may have already evaporated away. PBHs with mass $\sim 10^{12}$ kg and size of ~ 1 fm may still be present, and quite hot. Moss [2] has pointed out the possibility that a high-temperature symmetric phase can surround the black hole. Further away, the temperature drops and symmetry is broken. These symmetric and broken symmetric phases are separated by a domain wall which surrounds the black hole, i.e., the PBH lies within a "black hole bubble." A particle may have a mass m outside the bubble, while inside the bubble—in the symmetric phase—the particle mass vanishes by the Higgs mechanism. This particle will be totally reflected from the inner wall of the bubble if its energy is $E < m$, since it is energetically trapped. Trapped particles can help stabilize the bubble against collapse, and there can be an approach to a state of thermal equilibrium.

Recently, Green, Silverstein, and Starr [3] have conjectured that a different type of vacuum bubble, associated with scalar moduli fields sourced by matter fields of compact objects, may be catalyzed by evaporating black holes. A realization of this type of scenario leads to the possibility that such "moduli vacuum bubbles" may be end products of the Hawking radiation of black holes. These moduli vacuum bubbles can arise from the local effects of the matter sources coupling to one or more of the scalar moduli fields in the effective low-energy field theory.

Here we consider the possible effects of extra dimensions and the formation of a modulus vacuum bubble near a hot PBH by employing a model with one extra space dimension that is toroidally compactified, but in an inhomogeneous way. If the extra dimension has an associated scale factor $B(x^\mu)$, the physical size of the compact dimension is $(2\pi R_5)B(x^\mu)$, where R_5 is the radius of the compactified dimension. The 4D effective potential that arises from the extra dimension is temperature-dependent, and the equilibrium value of B may be quite different in the high- and low-temperature regions, so that the compactification is inhomogeneous. A modulus field $\varphi(x^\mu) \propto \ln B(x^\mu)$ can then give rise to the modulus bubble surrounding the PBH, with B interpolating between two different values on either side of the bubble wall. The bubble wall has a thickness δ and separates the hot region near the PBH and the cold asymptotic region. The presence of a domain wall with a variation in $B(x^\mu)$ over a distance δ can have dramatic effects on photons and other particles, and generally leads to energy-dependent reflectivities. For ordinary (nonmodulus) domain walls, reflection probabilities are relatively large for lower-particle energies $E \ll \delta^{-1}$, while transmission probabilities become large for higher energies $E \gg \delta^{-1}$. (See, e.g., Refs. [4–7].) The same type of behavior has been found for the case of domain walls associated with moduli [8]. Therefore, lower-energy particles can become trapped, at least to some degree, within a bubble and help to stabilize it against collapse.

If both types of bubble coexist—i.e., a modulus vacuum bubble and a nonmodulus false vacuum bubble from symmetry restoration at high temperature—there will be

*jmorris@iun.edu

a "double bubble" containing the PBH, interfering with the escape of various types of particles being emitted from it. The Hawking radiation will be partially trapped within the bubble, and to a distant observer an evaporating black hole may have a transmitted energy spectrum that is somewhat different from what would be expected from a black hole freely radiating into empty space, with the lower-frequency portions of the emission spectrum being suppressed. PBHs that have already evaporated away may have left metastable vacuum bubbles behind that contribute to the dark matter of the universe.

In Sec. II the effective 4D Einstein frame effective theory is obtained from the 5D theory. The form of the 4D effective potential U (developed in the appendices) for the scalar modulus containing contributions from one-loop quantum corrections at finite temperature, along with a cosmological constant, is presented, and the low- and high-temperature limits of U are examined. In Sec. III we consider black hole bubbles, both the (nonmodulus) symmetry-breaking (SB) type and the modulus type. A brief summary forms Sec. IV. In Appendix A the dependence of the effective potential U (for a flat Einstein frame) upon the Rubin-Roth action density and the cosmological constant is shown. Asymptotic forms of U are obtained in Appendix B.

II. EFFECTIVE 4D THEORY

Metric and effective action

We consider a 5D spacetime with a topology of $M_4 \times S^1$ having one toroidally compact extra dimension. The (mostly negative) 5D metric is $\tilde{g}_{MN}$:

$$ds^2 = \tilde{g}_{MN} dx^M dx^N = \tilde{g}_{\mu\nu} dx^\mu dx^\nu - B^2 dy^2 \tag{2.1}$$

where $M, N = 0, 1, 2, 3, 5$, $\mu, \nu = 0, 1, 2, 3$, and $y = x^5$ is the coordinate of the compact extra dimension, $0 \le y \le 2\pi R_5$. We allow $\tilde{g}_{\mu\nu}$ and $\sqrt{-\tilde{g}_{55}} = B$ to have a dependence on x^μ, but assume them to be independent of y. We also assume that $\tilde{g}_{\mu 5} = 0$. The scale factor $B(x^\mu)$ can be related to a scalar (modulus) field $\varphi(x^\mu)$ and the circumference of the extra dimension $L_5 = (2\pi R_5)\sqrt{-\tilde{g}_{55}}$ by

$$B = e^{\sqrt{2/3}\kappa\varphi}, \qquad \varphi = \frac{1}{\kappa}\sqrt{\frac{3}{2}}\ln B, \qquad L_5 = (2\pi R_5)B \tag{2.2}$$

where $\kappa = \sqrt{8\pi G} = \sqrt{8\pi}/M_P$, with $M_P = 1/\sqrt{G}$ the Planck mass. We can talk in terms of the scalar field φ, the scale factor B, or the circumference of the extra dimension L_5 interchangeably. We will want to focus attention upon a 4D effective potential U (which can be regarded as a function of either φ, B, or L_5) which originates from the Rubin-Roth potential describing one-loop quantum corrections at finite temperature due to Casimir effects for bosons and fermions [9,10], along with a contribution from a 5D cosmological constant Λ. Although, by Eq. (2.2), this effective potential will take different functional forms when expressed in terms of φ or B, we will describe it simply as $U(\varphi)$, $U(B)$, or $U(L_5)$ when confusion is not likely to arise. At low temperatures, Blau and Guendelman [11] demonstrated that there are parameter ranges for the effective potential U, allowing an inhomogeneous compactification to occur, so that in the effective 4D theory the scalar field $\varphi(x^\mu)$ can be associated with a domain wall that smoothly connects two vacuum states. The resulting "dimension bubbles" have peculiar properties [12–14] and can be stabilized by the entrapment of massive particle modes and/or photons.

We start with a 5D action

$$\begin{aligned} S &= \frac{1}{2\kappa_5^2}\int d^5x\sqrt{\tilde{g}_5}\{\tilde{R}_5 - 2\Lambda + 2\kappa_5^2\mathcal{L}_5\} \\ &= \frac{1}{2\kappa^2}\int d^4x\sqrt{-\tilde{g}}B\{\tilde{R}_5 - 2\Lambda + 2\kappa^2\mathcal{L}\} \end{aligned} \tag{2.3}$$

where we have used the definitions $\kappa_5^2 = 8\pi G_5 = (2\pi R_5)\kappa^2$, $\mathcal{L} = (2\pi R_5)\mathcal{L}_5$, $\tilde{g}_5 = \det\tilde{g}_{MN}$, and $\tilde{g} = \det\tilde{g}_{\mu\nu}$. Also, $\tilde{R}_5 = \tilde{g}^{MN}\tilde{R}_{MN}$ is the 5D Ricci scalar built from $\tilde{g}_{MN}$. The 4D Jordan frame metric is $\tilde{g}_{\mu\nu}$, the $\mu\nu$ part of $\tilde{g}_{MN}$. We define a 4D Einstein frame metric $g_{\mu\nu}$ by $g_{\mu\nu} = B\tilde{g}_{\mu\nu} = e^{\sqrt{2/3}\kappa\varphi}\tilde{g}_{\mu\nu} = (L_5/2\pi R_5)\tilde{g}_{\mu\nu}$. The line element in Eq. (2.1) then becomes

$$\begin{aligned} ds^2 &= B^{-1}g_{\mu\nu}dx^\mu dx^\nu - B^2 dy^2 \\ &= e^{-\sqrt{2/3}\kappa\varphi}g_{\mu\nu}dx^\mu dx^\nu - e^{2\sqrt{2/3}\kappa\varphi}dy^2. \end{aligned} \tag{2.4}$$

Using (2.3) and (2.4), the 5D action is dimensionally reduced to an effective 4D Einstein frame action

$$\begin{aligned} S &= \int d^4x\sqrt{-g}\left\{\frac{1}{2\kappa^2}R + \frac{1}{2}(\nabla\varphi)^2 + e^{-\sqrt{2/3}\kappa\varphi}[\mathcal{L} - \Lambda/\kappa^2]\right\} \\ &\times \int d^4x\sqrt{-g}\left\{\frac{1}{2\kappa^2}R + \frac{3}{4\kappa^2B^2}(\nabla B)^2 + B^{-1}[\mathcal{L} - \Lambda/\kappa^2]\right\} \end{aligned} \tag{2.5}$$

where $R = g^{\mu\nu}R_{\mu\nu}$ is the 4D Einstein frame Ricci scalar built from $g_{\mu\nu}$.

From (2.5) we see that in the effective 4D theory the extra dimensional scale factor enters as a scalar field and that there is a 4D effective Lagrangian $\mathcal{L}_4 = B^{-1}\mathcal{L}$ produced by the Lagrangian $\mathcal{L}$. A total effective 4D Lagrangian can therefore be written as

$$\mathcal{L}_{\text{eff}} = \frac{1}{2\kappa^2}R + \frac{1}{2}(\nabla\varphi)^2 - U(\varphi) + \mathcal{L}_4 \tag{2.6}$$

where $U(\varphi)$ is an effective potential that is constructed from one-loop quantum corrections for fermions and bosons at finite temperature (Rubin-Roth potential), along with the cosmological constant term.

The temperature-dependent effective potential U can be written in terms of L_5 and β, and its basic structure (expressed in a flat Einstein frame spacetime background) showing its dependence upon the Rubin-Roth potential $\tilde{\Gamma}$ and the cosmological constant Λ is given by (A17) in Appendix B. The result is

$$U(L_5, \beta) = (2\pi R_5)^2 \frac{\tilde{\Gamma}(L_5, \beta)}{\beta L_5^2} + (2\pi R_5) \frac{\Lambda/\kappa^2}{L_5}. \quad (2.7)$$

The asymptotic forms of $\tilde{\Gamma}$ for low and high temperatures are given in Tables I and II (taken from Table I in Ref. [10]). Using these we can express $U(L_5, \beta)$ for high- and low-β limits. These limiting forms (see Eqs. (B9) and (B10) in Appendix B) are given by

$$U \approx \begin{Bmatrix} [(N_f + n_f) - (N_b + n_b)](2\pi R_5)^2 \frac{3\zeta(5)}{4\pi^2} \frac{1}{L_5^6} + \frac{(2\pi R_5)\Lambda}{\kappa^2 L_5}, & L_5 \ll 1/M \\ (n_f - n_b)(2\pi R_5)^2 \frac{M^2}{4\pi^2} e^{-ML_5} \frac{1}{L_5^4} + \frac{(2\pi R_5)\Lambda}{\kappa^2 L_5}, & L_5 \gg 1/M \end{Bmatrix} \quad (\text{low } T) \quad (2.8)$$

for the high-β limit, where M is a typical particle mass parameter, and

$$U \approx \left[\left(N_b + \frac{15}{16} N_f\right)(2\pi R_5)^2 \frac{3\zeta(5)}{4\pi^2}\right] \frac{1}{\beta_1^5} \begin{Bmatrix} \frac{(N_f - N_b)}{(N_b + \frac{15}{16} N_f)} \frac{\beta_1^5}{L_5^6} + \frac{1}{L_5}, & L_5 \ll \beta \\ \left(1 - \frac{\beta_1^5}{\beta^5}\right) \frac{1}{L_5}, & L_5 \gg \beta \end{Bmatrix} \quad (\text{high } T) \quad (2.9)$$

for the low-β limit. Here, $n_{f(b)}$ = #massive fermionic (bosonic) modes, each of mass $\sim M$, and $N_{f(b)}$ = #effectively massless modes, with $N_b \geq 5$ (5 graviton degrees of freedom). We assume $N_f > N_b$ in (2.9) and $(N_f + n_f) - (N_b + n_b) > 0$ in (2.8). The parameter β_1 is defined by (see Eq. (B7))

$$T_1 = \frac{1}{\beta_1} = \left\{ \frac{\Lambda/\kappa^2}{(N_b + \frac{15}{16} N_f)(2\pi R_5) \frac{3\zeta(5)}{4\pi^2}} \right\}^{1/5}. \quad (2.10)$$

If we want to explicitly account for differences in particle masses in (2.8), we can make the replacement

$$n \frac{M^2}{4\pi^2} \frac{e^{-ML_5}}{L_5^4} \to \sum_i n^{(i)} \frac{M_i^2}{4\pi^2} \frac{e^{-M_i L_5}}{L_5^4} \quad (2.11)$$

with the index i running over the different species. The expression for U in terms of the scalar field φ is obtained by simply replacing L_5 by $(2\pi R_5) e^{\sqrt{2/3}\kappa\varphi}$.

We consider three distinct temperature ranges: a low-temperature (high $\beta = 1/T$) regime where $T \ll M$, where M is a typical particle mass; a high-temperature regime where $T \gg M$ but $T < T_1$; and a very high-temperature regime where $T \gg M$ and $T > T_1$.

The precise form of the effective potential depends upon the values of the various parameters, such as the 5D cosmological constant Λ and the compactification radius R_5, which are not known, but we consider (as in Refs. [11,12]) the interesting case for which the low temperature potential U has a local minimum at some value $L_5 = L_{5,\min}$ ($\varphi = \varphi_{\min}$), a local maximum at $L_5 = L_{5,\max} > L_{5,\min}$, and $U \to 0$ as $L_5 \to \infty$. There are then two low-energy states, at $L_{5,\min}$ and $L_5 > L_{5,\max}$, separated by a potential barrier. A scalar field domain wall solution φ interpolating between these two low-temperature "vacuum" states forms the wall of a low-temperature "dimension bubble" [11,12]. A schematic depiction of $U(L_5, \beta)$ for low T is sketched in Fig. 1. (We will later argue that the existence of a local minimum in the low-temperature potential, though required for the existence of a dimension bubble, is not required for the existence of a black hole modulus bubble.)

One can actually distinguish between two different possible types of low-temperature dimension bubble [14]. A type I bubble has a large value of L_5 in its interior and $L_5 \to L_{5,\min}$ outside the bubble. A type II bubble has $L_5 = L_{5,\min}$ in its interior and $L_5 > L_{5,\max}$ outside. In each case the bubble forms because $U_{\text{inside}} > U_{\text{outside}}$, causing the

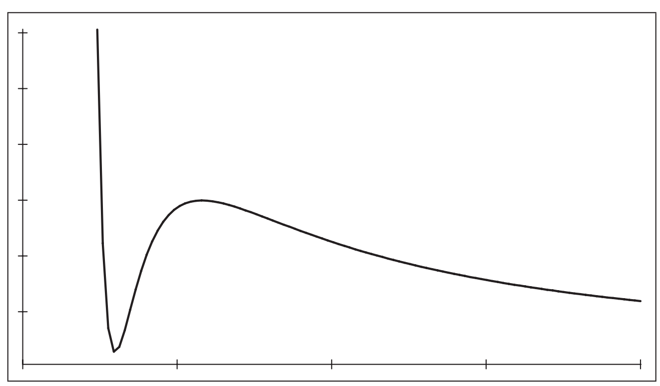

FIG. 1. Schematic depiction of U vs L_5 for low temperature.

domain wall to bend and enclose a region of higher energy density. Both types tend to entrap low-energy photons having wavelengths greater than the wall thickness. The photon and particle reflectivity from the bubble wall increases with an increasing difference between the values of L_5 (or φ) between the inside and outside of the bubble [8], so that photons and massive particle modes with energies $E \ll \delta^{-1}$ inside either a type I or type II bubble are effectively trapped when L_5 varies greatly between these regions. The particle entrapment can help to stabilize these bubbles from collapsing due to the wall tension [12–14].

Now consider the high-temperature limit, with U represented by (2.9). We see that at short distances in the y direction the potential U is positive, but the long-distance behavior can be either positive or negative, depending upon the temperature. More precisely, for $L_5 \gg \beta$, the potential U is positive for lower temperatures, $\beta > \beta_1$, and becomes negative for higher temperatures, $\beta < \beta_1$.

At very high temperatures $\beta < \beta_1$, the positive portion of U at small $L_5 \ll \beta_1$ must join with the negative portion of U at large $L_5 \gg \beta_1$, and asymptotically approach zero as $L_5 \to \infty$, indicating the presence of a local minimum somewhere roughly in the vicinity where the small and large distance parts of U join. We assume the minimum to be roughly located around $L_5 \sim O(\beta_1)$.

On the other hand, at lower temperatures $\beta > \beta_1$, the potential has positive short-distance and long-distance behaviors, and we infer that U is a positive monotonically decreasing function of L_5. Also notice that at the temperature $\beta = \beta_1$ the potential becomes flat at large L_5 distances. Schematic representations of these basic behaviors are indicated in Fig. 2.

Our basic view of the behavior of $U(L_5, \beta)$ from all this is something like the following: As the temperature T of the system increases, the barrier in the low-temperature potential shrinks and disappears, and consequently the state characterizing the system (the expectation value of L_5) may tend to roll outward toward larger values of L_5. However, as the temperature approaches $T_1 = 1/\beta_1$ the potential flattens out and a lower-energy minimum starts to appear at higher temperature, $T > T_1$, so that the state of the system rolls back inward toward this minimum, eventually settling into this very high-temperature vacuum state.

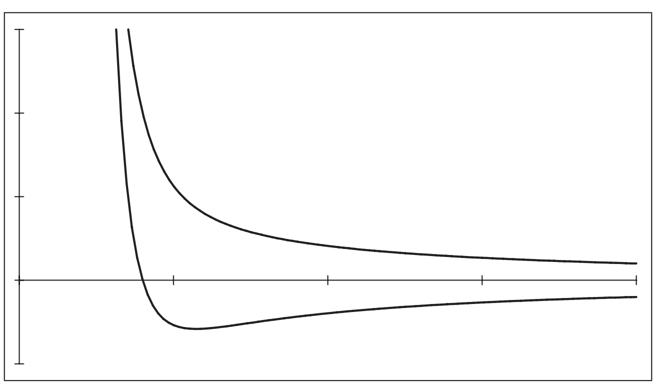

FIG. 2. Schematic depictions of U vs L_5 for high temperature $T < T_1$ (upper curve) and for very high temperature $T > T_1$ (lower curve).

III. BLACK HOLE BUBBLES

A. Modulus black hole bubble

For a black hole freely evaporating into empty space, the black hole temperature is

$$T_h = \frac{1}{8\pi G M_h} = \frac{1}{4\pi R_S} \tag{3.1}$$

where $R_S = 2GM_h$ is the Schwarzschild radius. The mass M_h of the black hole decreases at a rate $\dot{M}_h \propto -1/(GM_h)^2$, and consequently, PBHs with masses $M_h \lesssim 10^{12}$ kg would have evaporated away by now, and a PBH with mass $\sim 10^{12}$ kg and size of ~ 1 fm would be quite hot. Near such a PBH $\beta = 1/T$ is small, and far away from the PBH β is large. The effective potential $U(L_5, \beta)$, or $U(\varphi, T)$, would then vary with distance r from the hole, interpolating between the high-temperature and low-temperature forms described above. One then expects the vacuum expectation value (VEV) of L_5, B, and φ to vary with r. From Eq. (2.6) we have

$$\Box\varphi + \frac{\partial U(\varphi, T)}{\partial \varphi} - \frac{\partial \mathcal{L}_4}{\partial \varphi} = 0. \tag{3.2}$$

We can think of this variation in $\varphi(r)$ away from the PBH in terms of a black hole bubble [2,3] that surrounds the PBH as the scalar field passes through a range of values, as would the scalar field of a domain wall connecting two different vacuum states. The energy density of the bubble wall depends upon the kinetic and potential contributions from φ, and the thickness of the wall depends upon how rapidly the energy density varies. A thin-walled bubble would have a scalar field φ changing rapidly over a small distance, whereas a thick-walled bubble would have a more slowly varying field changing over a larger distance. Let us refer to this type of black hole bubble, formed by the scalar modulus φ, simply as a "modulus bubble" to distinguish it from an SB black hole bubble of the type originally described by Moss [2] that arises from the symmetry restoration near the PBH for a nonmodulus scalar field.

The forms of the effective potential given by (2.8) and (2.9) imply the existence of a modulus bubble when the interior temperature exceeds T_1, i.e., $\beta < \beta_1$, provided that

$$\begin{aligned} &1)\ T_1 < T_h = \frac{1}{8\pi G M_h},\ \text{i.e. } \beta_1 > \kappa^2 M_h = 4\pi R_S \qquad (\Lambda > 0)\\ &2)\ N_f - N_b > 0 \text{ at high } T \quad \text{and}\\ &3)\ n_f > n_b \quad \text{and,} \quad (N_f + n_f) > (N_b + n_b) \text{ at low } T. \end{aligned} \tag{3.3}$$

(Conditions 2 and 3 seem natural, with the number of fermionic modes exceeding the number of bosonic ones.) Condition 1 in (3.3) imposes a constraint upon the parameters Λ/κ^2 and $2\pi R_5$ by (2.10), namely,

$$\frac{\Lambda/\kappa^2}{(N_b + \frac{15}{16}N_f)(2\pi R_5)\frac{3\zeta(5)}{4\pi^2}} < \left(\frac{1}{\kappa^2 M_h}\right)^5 = \left(\frac{1}{4\pi R_S}\right)^5 \quad (3.4)$$

or

$$2\pi R_5 > \frac{(\Lambda/\kappa^2)(4\pi R_S)^5}{(N_b + \frac{15}{16}N_f)\frac{3\zeta(5)}{4\pi^2}}. \quad (3.5)$$

When these conditions in (3.3) hold, the minimum of U near the hole is negative, with $\varphi = \varphi_1$, say, and at asymptotic distances from the hole ($r \to \infty$, $T \to 0$) U is nonnegative in (2.8) with $\varphi \to \varphi_2$ asymptotically. Then, whether a local minimum of the low-temperature effective potential exists or not, φ must interpolate between the values φ_1 and φ_2 with an associated variation in U and a nonzero kinetic contribution from φ. The kinetic and potential terms contribute to the energy-momentum tensor $T^{(\varphi)}_{\mu\nu}$. The tensor $T^{(\varphi)}_{\mu\nu} \to 0$ as $r \to \infty$, so that the energy density of the modulus field is concentrated around the hole. The exact structure of the bubble, as well as its possible temporal evolution, are dictated by the solution to (3.2). Without a solution for $\varphi(r, t)$, the bubble wall characteristics, such as wall thickness δ, are undetermined, but will depend upon the length parameters β_1 and $2\pi R_5$. By choosing the asymptotic scale factor $B(\infty) = B_0 = 1$, then the asymptotic size of the extra dimension is $L_5(\infty) = 2\pi R_5$, which must be large enough to satisfy the constraint of (3.5) for a PBH with a given mass M_h and size R_S.

We can make a rough estimate of the right-hand side of (3.5) for a PBH with $R_S \sim 1$ fm $\sim .2$ GeV^{-1} using a current value of the cosmological constant for which $\Lambda/\kappa^2 \sim 10^{-47}$ GeV^4. Using $(N_b + \frac{15}{16}N_f) \sim 100$, Eq. (3.5) gives $2\pi R_5 > 10^{-41}$ GeV^{-1}, but this is automatically satisfied for these parameter choices if we require that $2\pi R_5$ be larger than the Planck length $l_P \sim 10^{-19}$ GeV^{-1}.

A rapidly varying φ could have a pronounced effect upon both the massive and massless particle modes of the radiation emitted by the evaporating black hole. The particle mass of a (Kaluza-Klein zero mode) boson or fermion in the effective 4D theory is given [12,14] by $m = B^{-1/2}(\varphi)M$, where M is the mass parameter in the original 5D theory. Therefore, in a region where φ and B decrease with r, the mass m increases with r, and there is a radially inward attractive force $\vec{F} \sim -\nabla m$ tending to decelerate a particle moving radially outward. The particle can become trapped in a region of higher φ if it has insufficient energy to escape. One has the reverse situation if φ increases with r, i.e., a particle would tend to be accelerated outward, again toward the region with larger φ and smaller m. This result also holds for the Kaluza-Klein excitation modes (see [14]). Whatever the classical particle motion, the probability that the particle escapes through the wall depends upon the magnitude of the variation in B across the wall [8]. Even if a particle is accelerated radially outward, it may be reflected back by the wall, with the probability of reflection being given by the reflection coefficient $\mathcal{R}$. (The coefficient $\mathcal{R}$ is independent of which side is the incident side.)

The effect of a varying φ upon photon propagation was investigated in [8,13]. An electromagnetic contribution to the effective 4D theory of the form $-\frac{1}{4}\varepsilon(\varphi)F^{\mu\nu}F_{\mu\nu}$ can be treated with a dielectric approach where a dielectric function, or permittivity, in a region of space is defined by $\varepsilon(\varphi) = B(\varphi)/B_0$, with B_0 being a constant (perhaps asymptotic) value of the scale factor B. The permeability is $\mu = 1/\varepsilon$ so that the index of refraction in a region of space is $n = \sqrt{\varepsilon\mu} = 1$ and the "impedance" is $Z = \sqrt{\mu/\varepsilon} = 1/\varepsilon \propto B^{-1}(\varphi)$. At a sharp boundary between two different constant values of B (thin-wall approximation) the reflection coefficient is given by [8,13]

$$\mathcal{R} = \left(\frac{\varepsilon_2 - \varepsilon_1}{\varepsilon_1 + \varepsilon_2}\right)^2 = \left(\frac{B_2 - B_1}{B_1 + B_2}\right)^2 \quad (3.6)$$

where $\varepsilon_{1,2}$ are the permittivity on the two different sides of the wall. This result holds for all angles of incidence and for light incident upon either side of the boundary. When the value of $B(\varphi)$ changes drastically across the boundary ($B_2 \ll B_1$ or $B_2 \gg B_1$) the magnitude of the reflection coefficient approaches unity, $|\mathcal{R}| \sim 1$. So for a thin-walled bubble where B varies drastically across the wall from one approximately constant value to another, the bubble wall is essentially opaque to photons. Photons inside the bubble would be trapped inside, and would only slowly leak out. The photon pressure would be exerted radially outward acting to counterbalance the inward pressure due to the bubble wall tension. For a thick bubble wall, where the photon wavelength is small compared to wall thickness, $\lambda \ll \delta$, the results obtained for ordinary (nonmodulus) domain walls [4–7] lead us to expect that $\mathcal{R}$ becomes small, with $\mathcal{R} \to 0$ as $\lambda \to 0$. This was indeed found to be the case in Ref. [8]. We therefore expect an entrapment of "low-energy" ($\omega \lesssim \delta^{-1}$) photons inside the bubble, while "high-energy" ($\omega \gtrsim \delta^{-1}$) photons escape. The same qualitative statements hold for the case of massive particle modes [8], and in the case that one side of the wall becomes kinematically inaccessible to sufficiently low-energy particles (say, $E < m_1$ or $E < m_2$), there is a total reflection from the wall.

We form the following rough picture for a modulus black hole bubble. Near the horizon of a very hot PBH ($T \gtrsim T_1$) we envision the VEV associated with L_5 to be on the order of $\beta_1 = 1/T_1$ with an associated scale factor $B_1 = L_5/(2\pi R_5) \sim O(\beta_1)/(2\pi R_5)$. However, asymptotically T approaches a value $L_5(\infty) = 2\pi R_5$ for $B(\infty) = B_0 = 1$. The ratio $B_{hor}/B_0 \sim B_1/B_0 \sim O(\beta_1)/(2\pi R_5) \gtrsim R_S/R_5$ depends on the value of β_1. With a large change in $B(\varphi)$ we have a black hole bubble forming around the PBH which tends to trap lower-energy photons and massive particles inside, due to a large reflection coefficient $\mathcal{R}$, which by (3.6) can be near unity. Massive particles that are kinematically forbidden to escape are totally reflected. However, for higher-energy modes with energies $E \gg \delta^{-1}$, the reflectivity becomes small and particles escape. The decrease in $\mathcal{R}$ becomes pronounced at an energy $E \sim \delta^{-1}$ [8]. The structure and evolution of the bubble require information about the bubble unavailable to us, and can only be described qualitatively, at best. For instance, it would be of interest to know the rate of photon and particle reabsorption by the black hole and the backreaction effects on the PBH evaporation. Also, as pointed out by Moss [2], there seems to be an intermediate case here between a black hole radiating freely into empty space and a black hole in thermal equilibrium. At any rate, there appears to be a strong possibility that the low-energy ($E \ll \delta^{-1}$) photon and particle components of the PBH thermal spectrum will not be observed asymptotically, whereas the high-energy particles ($E \gg \delta^{-1}$) will penetrate the modulus bubble wall. The presence of a modulus black hole bubble will therefore alter the emission spectrum seen by an outside observer.

The possibility might be entertained that a PBH that has evaporated away leaves behind a modulus bubble filled with various types of particles. The tendency for the bubble to shrink is countered by the particle pressure exerted outward on the bubble wall. The characteristics and evolution of a thin-walled bubble with an interior temperature T, with a particle energy density dominated by the effectively massless radiation modes, is expected to resemble those previously described for radiation-filled dimension bubbles [14]. There the bubble mass $\mathcal{M}$ depends on the particle radiation energy density $\rho_{\rm rad} = AT^4$, the φ-dependent interior energy density λ, the wall tension σ, and the bubble radius R_B. The minimization of $\mathcal{M}$ determines the equilibrium bubble size and mass. In [14] these were found for a stable bubble to be given by

$$R_B = \frac{6\sigma}{(\rho_{\rm rad} - 3\lambda)}, \qquad \mathcal{M} = 12\pi\sigma R_B^2\left(\frac{\rho_{\rm rad} - \frac{1}{3}\lambda}{\rho_{\rm rad} - 3\lambda}\right) \tag{3.7}$$

provided that $\rho_{\rm rad}/3 > \lambda$.

B. Symmetry-breaking black hole bubble

The SB black hole bubble proposed by Moss [2] arises from a high-temperature region near the PBH entering a symmetric phase with a Higgs field VEV $\phi = 0$ bounded by a broken symmetric phase farther away where $\phi \neq 0$. The bubble is bounded by a domain wall that separates these two phases. We then have the possibility that, due to the Higgs mechanism, particles can be massless in the high-T symmetric phase inside the bubble, but have nonzero rest mass m outside the bubble. Lower-energy particles emitted by the PBH with $E < m$ would become trapped inside and tend to resist the shrinkage of the bubble. More generally, particles incident upon the bubble wall typically suffer some degree of reflection from the wall. The reflection probability is expected to be larger for lower-energy particles (wave length $\gg$ wall thickness) and smaller for high-energy particles (wave length $\gg$ wall thickness). (See, e.g., Refs. [5–7].)

Photons are not trapped by the same dynamical mechanism, however, as they are massless in both phases. However, photons can be reflected from a bubble domain wall that is built from an isodoublet scalar field, as in electroweak theory, where one scalar component picks up a nonzero VEV in the broken symmetric phase. When the mixing between the vector fields constituting the physical photon field changes across the domain wall, then photons are also found to suffer some degree of reflection from the wall. Again, relatively low-energy photons (wave length $\gg$ wall thickness) are strongly reflected and relatively high-energy photons (wave length $\ll$ wall thickness) are strongly transmitted [5–7].

Therefore the bubble wall prevents the immediate escape of some of the normally massive particles, and possibly photons (for domain walls built from nonisoscalar scalar fields). A pressure is exerted on the wall, tending to halt its collapse. Assuming the dynamical time scales associated with bubble equilibration to be short compared to the PBH evaporation time, the bubble reaches an equilibrium state where the forces acting on the wall are balanced. Moss conjectured that such a bubble would exhibit a γ-ray luminosity which could be enhanced at certain energies.

C. Double bubble

If particle theories based upon spontaneous symmetry breaking are correct, *and* if there exists one or more extra space dimensions that can be inhomogeneously compactified, then it seems reasonable to speculate that (for certain parameter ranges) *both* types of black hole bubbles may enclose a hot PBH. In other words, we envision a situation wherein at least a portion of the interior of one type of bubble coincides with the interior of the other type of bubble as well. The PBH is enclosed by a double bubble. In the inner portion of the double bubble the rest mass of a normally (low-temperature) massive particle vanishes, so that low-energy particles get trapped. But photons can also get trapped by a photon-opaque thin-walled modulus bubble with a large variation in the scale factor B across the wall. The double bubble can therefore provide a substantial pressure serving to stabilize the bubble against immediate collapse. The amount and distinctiveness of the radiation emerging from the black hole and bubble will then depend upon the characteristics of the bubble walls, black hole temperature and evaporation rate, and approach to thermal equilibrium. The end result could be a nonnegligible deviation from the predictions for a black hole freely radiating into empty space. Furthermore, if black hole bubbles are endpoints of the Hawking radiation, smaller mass PBHs that have already evaporated may have left behind metastable bubbles that have not yet decayed, which could contribute to the dark matter of the universe.

IV. SUMMARY

Primordial black holes of mass $M_h \gtrsim 10^{12}$ kg may still be present in the universe today, and some may be quite hot, depending upon the mass. The temperature of the plasma around a black hole decreases with distance away from it, so that for sufficiently high-temperature PBHs there can be a region of restored symmetry (e.g., electroweak symmetry) near the hole and a region of broken symmetry further away. These regions are separated by a domain wall which bounds an SB black hole bubble. The bubble wall is expected to possess a reflection coefficient which decreases with increasing particle energy, but for particles with subcritical energies the reflection from the wall back into the bubble is total. So some of the Hawking radiation is blocked from escaping the black hole bubble.

If there is an extra space dimension which is compactified, the compactification can become inhomogeneous near a hot PBH. For the model considered here with one extra space dimension compactified on a circle, the inhomogeneous compactification gives rise to a second type of black hole bubble (modulus black hole bubble) characterized by a scale factor $B = \sqrt{-\tilde{g}_{55}}$ which varies with distance, provided that the conditions listed in (3.3) are satisfied, i.e., for the portion of parameter space where Λ/κ^2 and $2\pi R_5$ are constrained by (3.5). When the values of B inside and outside the bubble wall vary greatly, the reflection coefficient $\mathcal{R}(E)$ can approach unity for particles and photons with energies $E \ll \delta^{-1}$, where the bubble wall width δ depends upon model parameters.

Both types of black hole bubble may be produced, so that the PBH is enclosed within a black hole double bubble. The double bubble walls can impede the passage of both massive and massless particles produced by the PBH from within, so that a pressure tends to build up within the bubble. The attendant description is necessarily qualitative and somewhat speculative, since the actual characteristics of the bubble walls, backreaction on the black hole through particle reabsorption, and approach to thermal equilibrium, etc. are model-dependent and unknown. However, we conclude that if particle theories based upon spontaneous symmetry breaking are correct and/or there exists one or more extra space dimension(s) that becomes inhomogeneously compactified near a hot PBH, then the spectrum of radiation coming from the black hole could be significantly disturbed from what is expected for a blackbody. The presence of black hole bubbles due to symmetry restoration and/or extra dimensions may effectively disguise or hide evaporating black holes. PBHs created with masses $M_h \lesssim 10^{12}$ kg that have already evaporated away may have left behind metastable black hole bubbles which, if still in existence, contribute to the dark matter of the universe.

ACKNOWLEDGMENTS

I thank Eduardo Guendelman for comments.

APPENDIX A: THE 4D EFFECTIVE POTENTIAL

The 4D effective potential $U(L_5, \beta)$ has a contribution from a cosmological constant Λ in the 5D theory, along with a contribution from the Rubin-Roth (RR) potential $\tilde{\Gamma}(L_5, \beta)$ for one-loop quantum corrections at finite temperature due to Casimir effects for bosons and fermions [9,10]. Actually $\tilde{\Gamma}(L_5, \beta)$ is a Euclidean action density for a 5D theory with a flat 4D Jordan frame (JF) spacetime. This can be translated to an action density $\tilde{S}(L_5, \beta)$ for a flat 4D Einstein frame (EF). The 4D RR potential $U_{RR}(L_5, \beta)$ can be extracted from $\tilde{\Gamma}(L_5, \beta)$ or $\tilde{S}(L_5, \beta)$ and the full 4D EF effective potential $U(L_5, \beta)$ is built from the U_{RR} and Λ pieces.

1. Rubin-Roth effective actions

Jordan and Einstein frames: The 5D spacetime is described by

$$ds^2 = \tilde{g}_{\mu\nu}dx^\mu dx^\nu - B^2 dy^2 = B^{-1} g_{\mu\nu}dx^\mu dx^\nu - B^2 dy^2. \tag{A1}$$

The 4D JF metric is $\tilde{g}_{\mu\nu}$ (the $\mu\nu$ part of $\tilde{g}_{MN}$), and the 4D EF metric is $g_{\mu\nu}$,

$$\tilde{g}_{\mu\nu} = B^{-1} g_{\mu\nu}, \qquad \tilde{g}_{55} = -B^2, \tag{A2}$$

and $\tilde{g}_5 = \det(\tilde{g}_{MN}) = (-\tilde{g}_4)(-\tilde{g}_{55}) = B^2(-\tilde{g}_4)$. So

$$\sqrt{\tilde{g}_5} = B\sqrt{-\tilde{g}_4} = B^{-1}\sqrt{-g_4}. \tag{A3}$$

There are two different spacetimes being considered here, one with a flat 4D JF and one with a flat 4D EF:

$$\text{flat JF: } \tilde{g}_{\mu\nu} = \eta_{\mu\nu}, \qquad \sqrt{-\tilde{g}_4} = 1, \qquad \sqrt{\tilde{g}_5} = B \tag{A4}$$

$$\text{flat EF: } g_{\mu\nu} = \eta_{\mu\nu}, \qquad \sqrt{-g_4} = 1, \qquad \sqrt{\tilde{g}_5} = B^{-1}. \tag{A5}$$

We want to relate the RR actions Γ, $\tilde{\Gamma}$ evaluated in a flat JF to the actions S, $\tilde{S}$ evaluated in a flat EF. Γ and S are effective Euclidean actions, and $\tilde{\Gamma}$ and $\tilde{S}$ are action (3-) densities, defined by

$$\tilde{\Gamma} = \frac{\Gamma}{\int d^3x}, \qquad \tilde{S} = \frac{S}{\int d^3x}. \tag{A6}$$

Denote the 5D Euclidean action measure by d^5x_E, with a Wick rotation of the t coordinate.

RR Effective Actions, Flat JF: Although we are interested in x^μ-dependent T and B, we treat them as constant parameters in the evaluation of the effective action. For a flat JF we use $\sqrt{\tilde{g}_5} = B$. Introduce a 5D effective potential V_5 (see, e.g., Appelquist-Chodos [15]), and write a 5D effective action

$$\Gamma = V_5 \int d^5x_E \sqrt{\tilde{g}_5} = BV_5 \int_0^\beta d\tau \int_0^{2\pi R_5} dy \int d^3x = \int d^3x \tilde{\Gamma}, \tag{A7}$$

so that, with $L_5 \equiv (2\pi R_5)B$, we have

$$\tilde{\Gamma} = \beta L_5 V_5, \qquad V_5 = \frac{\tilde{\Gamma}}{\beta L_5}. \tag{A8}$$

The $\tilde{\Gamma}$ are the effective actions given by Rubin and Roth for one-loop quantum effects at finite T. They are obtained for a flat Jordan frame spacetime. For the ($N_B = 5$) graviton degrees of freedom in the zero temperature ($\beta \to \infty$) limit, from (A8) and the RR effective potential $\tilde{\Gamma}$ we recover the Appelquist-Chodos potential [15], V_{AC}, i.e.,

$$V_5 = \frac{\tilde{\Gamma}}{\beta L_5} = \frac{1}{\beta L_5}\left(-\frac{15}{4\pi^2}\zeta(5)\frac{\beta}{L_5^4}\right) = -\frac{15}{4\pi^2}\zeta(5)\frac{1}{L_5^5} = V_{AC}. \tag{A9}$$

RR Effective Actions, Flat EF: For a flat EF we use $\sqrt{\tilde{g}_5} = B^{-1}$, $\sqrt{-g_4} = 1$. Denote the effective action in this space by S, and the density by $\tilde{S} = S/\int d^3x$. Then

$$S = V_5 \int d^5x_E \sqrt{\tilde{g}_5} = B^{-1} V_5 \int_0^\beta d\tau \int_0^{2\pi R_5} dy \int d^3x = \frac{\beta V_5 L_5}{B^2} \int d^3x. \tag{A10}$$

Therefore, from (A8)

$$\tilde{S} = \frac{\beta L_5}{B^2} V_5 = \frac{\tilde{\Gamma}}{B^2} = (2\pi R_5)^2 \frac{\tilde{\Gamma}}{L_5^2}. \tag{A11}$$

The density $\tilde{S}$ is the corresponding effective RR action density for a flat Einstein frame spacetime.

2. Form of the 4D effective potential $U(L_5, \beta)$

The 5D action is

$$S = \int d^5x \sqrt{\tilde{g}_5}\left\{\frac{1}{2\kappa_5^2}(\tilde{R}_5 - 2\Lambda) + \mathcal{L}_5\right\} = \int d^4x \sqrt{\tilde{g}_4} B\left\{\frac{1}{2\kappa^2}(\tilde{R}_5 - 2\Lambda) + (2\pi R_5)\mathcal{L}_5\right\} \tag{A12}$$

giving the dimensionally reduced 4D EF effective action

$$S = \int d^4x \sqrt{-g}\left\{\frac{1}{2\kappa^2}R + \frac{3}{4\kappa^2}\left(\frac{\nabla B}{B}\right)^2 + B^{-1}\left[(2\pi R_5)\mathcal{L}_5 - \frac{\Lambda}{\kappa^2}\right]\right\}. \tag{A13}$$

The 4D EF effective Lagrangian arising from the $\mathcal{L}_5$ and Λ terms is

$$\mathcal{L}_{4,\mathrm{eff}} = B^{-1}\left[(2\pi R_5)\mathcal{L}_5 - \frac{\Lambda}{\kappa^2}\right]. \tag{A14}$$

We set $\mathcal{L}_5 = -V_5$, where V_5 is the 5D effective potential in (A8) and (A11), and then identify the 4D EF effective potential $\mathcal{L}_{4,eff} = -U$:

$$U = B^{-1}\left[(2\pi R_5)V_5 + \frac{\Lambda}{\kappa^2}\right] = U_{RR} + U_\Lambda, \tag{A15}$$

$$U_{RR} = B^{-1}(2\pi R_5)V_5, \qquad U_\Lambda = B^{-1}\frac{\Lambda}{\kappa^2} \tag{A16}$$

where the RR and Λ parts are combined to give the total potential U. The effective potential $U = U_{RR} + U_\Lambda$ can be written in terms of B or L_5:

$$U_{RR} = \frac{\tilde{\Gamma}}{\beta B^2} = (2\pi R_5)^2 \frac{\tilde{\Gamma}}{\beta L_5^2}$$
$$U_\Lambda = \frac{\Lambda/\kappa^2}{B} = (2\pi R_5)\frac{\Lambda/\kappa^2}{L_5} \tag{A17}$$
$$U(L_5, \beta) = (2\pi R_5)^2 \frac{\tilde{\Gamma}}{\beta L_5^2} + (2\pi R_5)\frac{\Lambda/\kappa^2}{L_5}.$$

TABLE I. Effective potential (action density) $\tilde{\Gamma}$ per degree of freedom for ultrarelativistic modes.

Effective potential $\tilde{\Gamma}$	Ultrarelativistic ($M \ll T$)	
Per degree of freedom	$L_5 \ll \beta \ll 1/M$	$\beta \ll L_5 \ll 1/M$ and $\beta \ll 1/M \ll L_5$
$\tilde{\Gamma}_b$	$-\frac{3\zeta(5)}{4\pi^2}\frac{\beta}{L_5^4}$ $\boxed{1}$	$-\frac{3\zeta(5)}{4\pi^2}\frac{L_5}{\beta^4}$ $\boxed{7}$
$\tilde{\Gamma}_f$	$\frac{3\zeta(5)}{4\pi^2}\frac{\beta}{L_5^4}$ $\boxed{2}$	$-\frac{3\zeta(5)}{4\pi^2}\left(\frac{15}{16}\right)\frac{L_5}{\beta^4}$ $\boxed{8}$

TABLE II. Effective potential (action density) $\tilde{\Gamma}$ per degree of freedom for nonrelativistic modes.

Effective potential $\tilde{\Gamma}$	Nonrelativistic ($M \gg T$)		
Per degree of freedom	$L_5 \ll 1/M \ll \beta$	$1/M \ll L_5 \ll \beta$	$1/M \ll \beta \ll L_5$
$\bar{\Gamma}_b$	$-\frac{3\zeta(5)}{4\pi^2}\frac{\beta}{L_5^4}$ $\boxed{3}$	$-\frac{M^2}{4\pi^2}\frac{\beta}{L_5^2}e^{-ML_5}$ $\boxed{5}$	$-\frac{M^2}{4\pi^2}\frac{\beta}{L_5^2}e^{-M\beta}$ $\boxed{9}$
$\bar{\Gamma}_f$	$\frac{3\zeta(5)}{4\pi^2}\frac{\beta}{L_5^4}$ $\boxed{4}$	$\frac{M^2}{4\pi^2}\frac{\beta}{L_5^2}e^{-ML_5}$ $\boxed{6}$	$-\frac{M^2}{4\pi^2}\frac{\beta}{L_5^2}e^{-M\beta}$ $\boxed{10}$

APPENDIX B: ASYMPTOTIC FORMS OF $U(L_5, \beta)$

1. Rubin-Roth part

Rubin and Roth have compiled a table (Table I in Ref. [10]) of effective potential contributions per degree of freedom for bosons and fermions (for untwisted and twisted fields). Here, we use only the untwisted contributions. Tables I and II list these contributions for the ultrarelativistic and nonrelativistic limits. The effective potential per degree of freedom is denoted here by $\bar{\Gamma} = \tilde{\Gamma}/(\text{degree freedom})$ and M refers to particle mass. (The table entries are numbered for use below.)

The following notation is used to label particle modes:

$$N_{b(f)} = \text{ number of effectively massless modes at temperature } T; \quad M \ll T, \beta \ll 1/M$$
$$n_{b(f)} = \text{ number of massive modes at temperature } T; \quad M \gg T, \beta \gg 1/M.$$

E.g., at low T the effectively massless modes may be the exactly massless modes (like graviton, photon), and very light fermions and scalars (like ν's); very massive modes would become relatively suppressed through factors like e^{-ML_5} and $e^{-M\beta}$. The various terms in Tables I and II are represented by $\bar{\Gamma}_i$ for term $\boxed{i}$.

2. Low-T limit ($T \to 0$)

We consider $T \approx 0$, $\beta \to \infty$, but finite. For effectively *massless modes*, $M \ll T$, $\beta \ll \frac{1}{M}$,

$$\bar{\Gamma} \sim \begin{Bmatrix} \text{terms } 1, 2 & (\bar{\Gamma}_1, \bar{\Gamma}_2), & L_5 \ll \beta \ll 1/M \\ \text{terms } 7, 8 & (\bar{\Gamma}_7, \bar{\Gamma}_8), & \beta \ll L_5 \ll 1/M \end{Bmatrix}$$

$$\tilde{\Gamma} \approx \begin{Bmatrix} (N_f - N_b)\frac{3\zeta(5)}{4\pi^2}\frac{\beta}{L_5^4}, & L_5 \ll \beta \ll 1/M \\ -(N_b + \frac{15}{16}N_f)\frac{3\zeta(5)}{4\pi^2}\frac{L_5}{\beta^4}, & \beta \ll L_5 \ll 1/M \end{Bmatrix},$$

$$M \ll T, \qquad \beta \ll \frac{1}{M}. \tag{B1}$$

For *massive modes*, $M \gg T$, $\beta \gg \frac{1}{M}$, ($\beta \to \infty$, but finite),

$$\bar{\Gamma} \sim \begin{Bmatrix} \text{terms } 3, 4 & (\bar{\Gamma}_3, \bar{\Gamma}_4), & L_5 \ll \frac{1}{M} \ll \beta \\ \text{terms } 5, 6 & (\bar{\Gamma}_5, \bar{\Gamma}_6), & \frac{1}{M} \ll L_5 \ll \beta \end{Bmatrix}$$

$$\tilde{\Gamma} \approx \begin{Bmatrix} (n_f - n_b)\frac{3\zeta(5)}{4\pi^2}\frac{\beta}{L_5^4}, & L_5 \ll \frac{1}{M} \ll \beta \\ (n_f - n_b)\frac{M^2}{4\pi^2}\frac{\beta}{L_5^2}e^{-ML_5}, & \frac{1}{M} \ll L_5 \ll \beta \end{Bmatrix},$$

$$M \gg T, \qquad \beta \gg \frac{1}{M}. \tag{B2}$$

Total $\tilde{\Gamma}$ for all modes at low T: add all of the $L_5 \ll \frac{1}{M}$ terms (but drop the bottom terms $\bar{\Gamma}_7, \bar{\Gamma}_8$ in (B1), since these terms $\to 0$ as $\beta \to \infty$) and add all of the $L_5 \gg \frac{1}{M}$ terms to get a total $\tilde{\Gamma}$ for small and large L_5 at low T:

$$\tilde{\Gamma} \approx \begin{Bmatrix} [(N_f + n_f) - (N_b + n_b)]\frac{3\zeta(5)}{4\pi^2}\frac{\beta}{L_5^4}, & L_5 \ll 1/M \\ (n_f - n_b)\frac{M^2}{4\pi^2}\frac{\beta}{L_5^2}e^{-ML_5}, & L_5 \gg 1/M \end{Bmatrix}$$

$$(\tilde{\Gamma} \text{ at low} T). \tag{B3}$$

3. High-T limit ($T \gg M$)

For the high-T limit ($T \gg M$, $\beta \ll \frac{1}{M}$) we consider only the ultrarelativistic effectively massless modes, as they dominate the massive ones for the asymptotic forms.

$$\bar{\Gamma} \sim \begin{Bmatrix} \bar{\Gamma}_1, \bar{\Gamma}_2, & (\text{small} L_5) L_5 \ll \beta \ll \frac{1}{M} \\ \bar{\Gamma}_7, \bar{\Gamma}_8, & (\text{large} L_5) L_5 \gg \beta \end{Bmatrix}$$

$$\tilde{\Gamma} \approx \begin{Bmatrix} (N_f - N_b)\frac{3\zeta(5)}{4\pi^2}\frac{\beta}{L_5^4}, & (\text{small} L_5) L_5 \ll \beta \\ -(N_b + \frac{15}{16}N_f)\frac{3\zeta(5)}{4\pi^2}\frac{L_5}{\beta^4}, & (\text{large} L_5) L_5 \gg \beta \end{Bmatrix}$$

$$(\Gamma_{RR} \text{ at high} T, T \gg M). \tag{B4}$$

4. Total effective potential

From (A17), (B3), and (B4), the asymptotic forms of the total effective potential U can be written out for the low- and high-temperature limits. For low T,

$$U \approx \left\{ \begin{matrix} [(N_f + n_f) - (N_b + n_b)](2\pi R_5)^2 \frac{3\zeta(5)}{4\pi^2} \frac{1}{L_5^6} + \frac{(2\pi R_5)\Lambda}{\kappa^2 L_5}, & L_5 \ll 1/M \\ (n_f - n_b)(2\pi R_5)^2 \frac{M^2}{4\pi^2} e^{-ML_5} \frac{1}{L_5^4} + \frac{(2\pi R_5)\Lambda}{\kappa^2 L_5}, & L_5 \gg 1/M \end{matrix} \right\} \quad (\mathrm{Low}T) \tag{B5}$$

where $N = $ #massless modes, $n = $ #of massive modes, each with mass $\sim M$. This U is β independent, $\beta \gg \frac{1}{M}$, with $T \rightarrow 0^+$, $\beta \rightarrow \infty$, but finite. For high T,

$$U \approx \left\{ \begin{matrix} [(N_f - N_b)](2\pi R_5)^2 \frac{3\zeta(5)}{4\pi^2} \frac{1}{L_5^6} + \frac{(2\pi R_5)\Lambda}{\kappa^2 L_5}, & L_5 \ll \beta \\ -(N_b + \frac{15}{16} N_f)(2\pi R_5)^2 \frac{3\zeta(5)}{4\pi^2} \frac{1}{\beta^5 L_5} + \frac{(2\pi R_5)\Lambda}{\kappa^2 L_5}, & L_5 \gg \beta \end{matrix} \right\} \quad (\mathrm{High}T) \tag{B6}$$

with $T \gg M$, $\beta \ll \frac{1}{M}$. (relativistic modes) We assume $N_f^{\mathrm{Tot}} > N_b^{\mathrm{Tot}}$ for all cases.

We can define the temperature parameters T_1 and β_1,

$$T_1 = \frac{1}{\beta_1} = \left\{ \frac{\Lambda/\kappa^2}{(N_b + \frac{15}{16} N_f)(2\pi R_5) \frac{3\zeta(5)}{4\pi^2}} \right\}^{1/5} \tag{B7}$$

which are real, provided that $\Lambda > 0$. There are three parameters, $(2\pi R_5)$, Λ/κ^2, and β_1, related by the definition of β_1, leaving two independent parameters, e.g., $(2\pi R_5)$ and β_1. The high T effective potential, in terms of β_1, is then

$$U \approx \left[\left(N_b + \frac{15}{16} N_f \right) (2\pi R_5)^2 \frac{3\zeta(5)}{4\pi^2} \right] \frac{1}{\beta_1^5} \left\{ \begin{matrix} \frac{(N_f - N_b)}{(N_b + \frac{15}{16} N_f)} \frac{\beta_1^5}{L_5^6} + \frac{1}{L_5}, & L_5 \ll \beta \\ (1 - \frac{\beta_1^5}{\beta^5}) \frac{1}{L_5}, & L_5 \gg \beta \end{matrix} \right\} \quad (\mathrm{high}T). \tag{B8}$$

5. Summary

The limiting forms for the temperature-dependent 4D effective potential $U(L_5, \beta)$ are given by

$$U \approx \begin{pmatrix} [(N_f + n_f) - (N_b + n_b)](2\pi R_5)^2 \frac{3\zeta(5)}{4\pi^2} \frac{1}{L_5^6} + \frac{(2\pi R_5)\Lambda}{\kappa^2 L_5}, & L_5 \ll 1/M \\ (n_f - n_b)(2\pi R_5)^2 \frac{M^2}{4\pi^2} e^{-ML} \frac{1}{L_5^4} + \frac{(2\pi R_5)\Lambda}{\kappa^2 L_5}, & L_5 \gg 1/M \end{pmatrix} \quad (\mathrm{low}T) \tag{B9}$$

$$U \approx \left[\left(N_b + \frac{15}{16} N_f \right) (2\pi R_5)^2 \frac{3\zeta(5)}{4\pi^2} \right] \frac{1}{\beta_1^5} \left\{ \begin{matrix} \frac{(N_f - N_b)}{(N_b + \frac{15}{16} N_f)} \frac{\beta_1^5}{L_5^6} + \frac{1}{L_5}, & L_5 \ll \beta \\ (1 - \frac{\beta_1^5}{\beta^5}) \frac{1}{L_5}, & L_5 \gg \beta \end{matrix} \right\} \quad (\mathrm{high}T) \tag{B10}$$

[1] S. W. Hawking, Nature (London) **248**, 30 (1974); Commun. Math. Phys. **43**, 199 (1975).
[2] I. G. Moss, Phys. Rev. D **32**, 1333 (1985).
[3] D. Green, E. Silverstein, and D. Starr, Phys. Rev. D **74**, 024004 (2006).
[4] A. Vilenkin and E. P. S. Shellard, *Cosmic Strings and Other Topological Defects* (Cambridge University Press, Cambridge, England, 1994).
[5] A. E. Everett, Phys. Rev. D **10**, 3161 (1974).
[6] A. Ayala, J. Jalilian-Marian, L. D. McLerran, and A. P. Vischer, Phys. Rev. D **49**, 5559 (1994).
[7] G. R. Farrar and J. W. McIntosh, Jr., Phys. Rev. D **51**, 5889 (1995).
[8] N. De Leon and J. R. Morris, Phys. Rev. D **74**, 045033 (2006).
[9] M. A. Rubin and B. D. Roth, Nucl. Phys. **B226**, 444 (1983).
[10] M. A. Rubin and B. D. Roth, Phys. Lett. B **127**, 55 (1983).
[11] S. K. Blau and E. I. Guendelman, Phys. Rev. D **40**, 1909 (1989).
[12] J. R. Morris, Phys. Rev. D **67**, 025005 (2003).
[13] E. I. Guendelman and J. R. Morris, Phys. Rev. D **68**, 045008 (2003).
[14] J. R. Morris, Phys. Rev. D **70**, 025007 (2004).
[15] T. Appelquist and A. Chodos, Phys. Rev. D **28**, 772 (1983).